IEEE Access
Multidisciplinary ⋮ Rapid Review ⋮ Open Access Journal

Received 17 April 2023, accepted 4 June 2023, date of publication 13 June 2023, date of current version 21 June 2023.

Digital Object Identifier 10.1109/ACCESS.2023.3285821

RESEARCH ARTICLE

Lung Cancer Classification Using Modified U-Net Based Lobe Segmentation and Nodule Detection

IFTIKHAR NASEER[1], SHEERAZ AKRAM[1,2,3], TEHREEM MASOOD[1,2], MUHAMMAD RASHID[4], AND ARFAN JAFFAR[1,2]

[1]Faculty of Computer Science and Information Technology, Superior University, Lahore 54000, Pakistan
[2]Intelligent Data Visual Computing Research (IDVCR), Lahore 55150, Pakistan
[3]Information Systems Department, College of Computer and Information Sciences, Imam Mohammad Ibn Saud Islamic University (IMSIU), Riyadh 12571, Saudi Arabia
[4]Department of Computer Science, National University of Technology, Islamabad 45000, Pakistan

Corresponding author: Iftikhar Naseer (iftikharnaseer@gmail.com)

ABSTRACT Lung cancer is the most common cause of cancer deaths worldwide. Early detection is crucial for successful treatment and increasing patient survival rates. Artificial intelligence techniques can play a significant role in the early detection of lung cancer. Various methods based on machine learning and deep learning approaches are used to detect lung cancer. This research works aims to develop automated methods to accurately identify and classify lung cancer in CT scans by using computational intelligence techniques. The process typically involves lobe segmentation, extracting candidate nodules, and classifying nodules as either cancer or non-cancer. The proposed lung cancer classification uses modified U-Net based lobe segmentation and nodule detection model consisting of three phases. The first phase segments lobe using CT slice and predicted mask using modified U-Net architecture and the second phase extracts candidate nodule using predicted mask and label employing modified U-Net architecture. Finally, the third phase is based on modified AlexNet, and a support vector machine is applied to classify candidate nodules into cancer and non-cancer. The experimental results of the proposed methodology for lobe segmentation, candidate nodule extraction, and classification of lung cancer have shown promising results on the publicly available LUAN16 dataset. The modified AlexNet-SVM classification model achieves 97.98% of accuracy, 98.84% of sensitivity, 97.47% of specificity, 97.53% of precision, and 97.70% of F1 for the classification of lung cancer.

INDEX TERMS AlexNet, nodule extraction, lung cancer, segmentation, support vector machine, U-Net.

I. INTRODUCTION

Lung cancer has a high incidence and death among all other cancers. Approximately 1,958,310 total new cancer cases and 609,820 cancer death are anticipated to occur in the United State of America in 2023 including 350 deaths daily from lung cancer [1]. An early lung cancer diagnosis can significantly reduce the mortality rate and approximately 54% increase in survival rate up to 5 years [2]. Image processing methods have been utilized to examine medical images for many years. The computer-aided diagnosis (CAD) system can provide a rapid, accurate, and efficient diagnosis of disease, which can help in the treatment of patients. Early detection of diseases become a major reason for to decline in death rate for various kinds of cancers such as breast cancer, kidney stones, brain cancer, blood cancer, stomach cancer, and lung cancer. In this regard, various research efforts have been done to aid and improve the diagnosis process of diseases from medical imagery [3].

Researchers have developed various segmentation frameworks or models to detect lung cancerous tumors to provide help to radiologists. Lung cancer segmentation methods are divided into two types: The first type comprises traditional techniques while the second type consists of deep learning (DL) techniques. Traditional techniques mostly centered on intensity-based methods such as region growing [4], [5],

The associate editor coordinating the review of this manuscript and approving it for publication was Jon Atli Benediktsson.

[6], adaptive threshold [7], [8], [9], [10], the morphological method [11], [12], active-contour model [12], [13], [14], and shape analysis [15], [16], [17]. However, these methods are not robust in the case of variation of tumor sizes as well as not appropriate for lung segmentation tumors. Moreover, in these methods, when the tumors are attached to the other organs, the performance of tumor segmentation methods affects the level of automation, which is consequently low. Therefore, some lung tumor segmentation methods might be misguided [18]. Therefore, traditional methods are being replaced by deep convolutional neural network (DCNN) models. Existing deep learning techniques have outperformed several image recognition problems. DL techniques can efficiently extract important features optimally without human participation. These techniques can improve accuracy in the detection of various diseases in the medical field. Numerous imaging modalities such as X-Rays, magnetic resonance imaging (MRI) positron emission tomography (PET), and computed tomography (CT) have been applied to detect pulmonary nodules [19]. The researchers are applying deep learning techniques such as CSE-GAN [20], MSU-Net [21], dual-branch residual network(DB-ResNet) [22], 3D-UNet [23], MSDS-U-Net [24], DS-CMSF [25], dual-path lung nodules segmentation based on boundary enhancement and hybrid transformer (DPBET) [26], DAS-NET [27], Lung PAYNet [28], LungNet-SVM [29] to improve the segmentation task in medical images. The mentioned networks apply benchmark U-Net architecture and obtained different level of accuracy but still, there is a need to improve the accuracy of the segmentation process.

Image segmentation divides an image into different image objects and boundaries. Medical image segmentation plays a decisive role in the detection of several diseases through deep learning methods. Automated segmentation methods based on CT and MRI have increased in demand [30]. Deep learning networks mostly used encoder-decoder architectures and deep generative models for medical image segmentation. The U-Net-based model crops the feature maps from the encoding component, copy them to the decoding component, and for segmentation map generation [31]. Pulmonary cancer nodules are detected by various researchers using different segmentation methods. Deep learning-based CAD solutions can decrease the burden of medical experts to detect various diseases particularly segmentation, detection, and classification of lung cancer nodules. This research presents an automatic deep learning-based model that segments, detects, and classifies lung nodules increases the accuracy rate, and reduces false positives while detecting lung nodules. Eventually, lung cancer detection at an early stage will reduce the mortality rate.

II. LITERATURE REVIEW

Pulmonary nodule detection is a crucial task and early detection of lung cancer is needed to reduce the mortality rate and appropriate treatment. Various computational techniques are used to detect lung cancer and several research methods have been reported in the literature. Therefore, we have analyzed the techniques below including segmentation, classification, and detection of lung cancerous nodules.

In medical imaging, deep convolutional neural networks (DCNN) made fabulous achievements. Shelhamer et al. [32] presented an end-to-end network based on a fully convolutional network which is more accurate for image segmentation. Ronneberger et al. [33] introduced U-Net architecture consisting of encoder-decoder and skip connection used to retain important information from the different sizes of feature maps and attained remarkable performance in medical image segmentation tasks. Singadkar et al. [34] used a deep deconvolutional residual network (DDRN) in the 2D CT lung images for automatic lung nodule segmentation and this model was end-to-end trained with fully captured resolution features. Fu et al. [35] introduced a multi-task learning model consisting of a convolutional neural network (CNN) to segment 2D CT images. Their model used an arbitrary depth technique on entire nodule volumes and a slice attention module applied to drop irrelevant slices. Moreover, attribute and cross-attribute modules represented meaningful relationships between attributes. Bruntha et al. [28] suggested an inverted residual block used by the encoder and decoder to segment lung nodules. In their proposed Lung PAYNet architecture, they applied a pyramid attention network to extract dense features from the encoder and decoder. According to Liang et al. [36] segmentation uncertainty at the pulmonary nodule boundary is considered a challenge and to overcome this challenge the authors presented Uncertainty Analysis Based Attention UNet (UAA-UNet) model. The proposed network deals with uncertainty in edge regions and it contains two stages. In the first stage, initial segmentation maps of pulmonary nodules were found and uncertainty regions are focused on in the second step. A UAA UNet model has achieved a sensitivity of 85.11% and Dice of 86.89% for nodule segmentation. Wang et al. [37] have designed a selective kernel V-Net architecture for the extraction of multi-scale feature information and improved lung nodule segmentation performance with Dice of 0.796, Jaccard of 0.665, and 0.789 sensitivity. He and Li [38] presented an ISHAP (Improved SHapley Additive exPlanations)-based model to classify lung nodules. Medical prior knowledge was used to extract semantic and radiomics features. ISHAP explanation and recursive feature elimination algorithm were applied to guide important features and classifiers with parameters. Then, the ISHAP-based model utilized to classify pulmonary nodules into cancer and non-cancer on the LIDC dataset obtained 0.873 of accuracy, 0.885 of specificity, and 0.862 of sensitivity. Huidrom et al. [39] focused neuro-evolutional approach containing a feed-forward neural network for the detection of pulmonary nodules. This method worked with particle swarm optimization and cuckoo search algorithm and yielded 95.5% of accuracy and 95.8% of sensitivity. Similarly, another research presented by [40] to detect lung cancer detection based on CNN and gen-

TABLE 1. Limitation of previous work.

Publications	Year	Dataset	Methods	Accuracy (%)	Limitation
Halder et al. [15]	2022	LIDC-IDRI	2- Pathway Morphology-based Convolutional Neural Network (2PMorphCNN)	96.10	Lack of Transparency
Fu et al. [35]	2022	LIDC-IDRI	convolutional neural network (CNN)-based MTL model	94.7	Need to improve accuracy
Huidrom et al. [39]	2022	LUNA16	Neuro-evolutional approach	95.5	Hand crafted features
Suresh et al. [40]	2020	LIDC-IDRI	CNN and generative adversarial networks (GANs)	93.9	Need to improve accuracy
Li et al. [41]	2019	LIDC-IDRI	Handcrafted features and CNN based algorithm	93.07	Hand crafted features
Bhaskar et al. [44]	2022	LUNA16	Multi- scale Laplacian of Gaussian filters and Deep CNN	93.2	Need to improve accuracy
Han et al. [45]	2022	LUNA16	3D ResNet	91.1	Need to improve accuracy
Bruntha at al. [46]	2022	LIDC-IDRC	Hybridized Feature Extraction Approach	97.53%	Hand crafted features
Al-Shabi et al. [47]	2022	LIDC-IDRI	Progressive Growing Channel Attentive Non-Local (ProCAN) network	94.11	Need to improve accuracy
Huang et al. [48]	2022	LIDC-IDRI	Deep feature optimization framework (DFOF)	92.13%	Need to improve accuracy
Dodia et al. [50]	2022	LUNA16	Elagha initialization-based Fuzzy C-Means clustering (EFCM)	94.87	Need to improve accuracy Limited generalizability to other datasets
Lye et al. [51]	2020	LIDC-IDRI	multi-level cross residual convolutional neural network (ML-xResNet)	92.19	Need to improve accuracy

erative adversarial networks (GANs). Li et al. [41] used handcrafted features followed by the convolutional neural network. Nageswaran et al. [42] presented a lung cancer classification technique using various machine learning (ML) methods such as artificial neural network (ANN), K-nearest neighbors (KNN), and random forest. Nodule classification was performed by Zhao et al. [43] which consisted of an attentive module that scratches spatial and global information. Furthermore, multilevel contextual information encoded by the adaptive conv-kernels method improved nodule classification accuracy. Bhaskar and Ganashree [44] introduced an effective method using multi-scale Laplacian of Gaussian filters and deep convolutional neural network to detect pulmonary nodules and achieved 71.2% recall, and 93.2% accuracy.

Han et al. [45] detected and classified lung nodules by applying a 3D ResNet algorithm and a fully connected neural network to reduce the medical expert's workload on the LUNA16 dataset. Similarly, Bruntha et al. [46] used ResNet50 and a handcrafted histogram of oriented gradient (HOG) for deep feature extraction and handcrafted feature respectively. A support vector machine (SVM) was used to classify non-cancer and cancer nodules for this proposed hybridized model on the LIDC dataset. Al-Shabi et al. [47] introduced a model for lung nodule classification namely Progressive Growing Channel Attentive Non-Local (ProCAN) network reached an accuracy of 95.28%. Huang et al. [48] introduced an effective model based on a deep feature optimization framework (DFOF) for lung cancer classification. The model yielded 92.13% accuracy and 87.16%. recall and 94.16% precision.

Mahmood and Ahmed [49] introduced an automatic CAD system based on AlexNet architecture to classify lung nodules. The proposed AlexNet architecture was tuned with several layers and hyperparameters to achieve superior performance. The model achieved results of the pulmonary cancer screening trial were 98.9% of specificity and 98.7% of accuracy. Another research work by Dodia et al. [50], presented an elagha initialization-based fuzzy c-means clustering (EFCM) and SVM presented for segmentation and detection of nodules respectively. Lyu et al [51] suggested a model based on a multi-level cross-residual network (ML-xResNet) to classify the lung nodules and achieved 92.19% of accuracy.

The major limitation of previous studies is shown in Table 1.

Table 1 is showing some limitations of the previous studies included hand crafted features [39], [41], [46], the need to

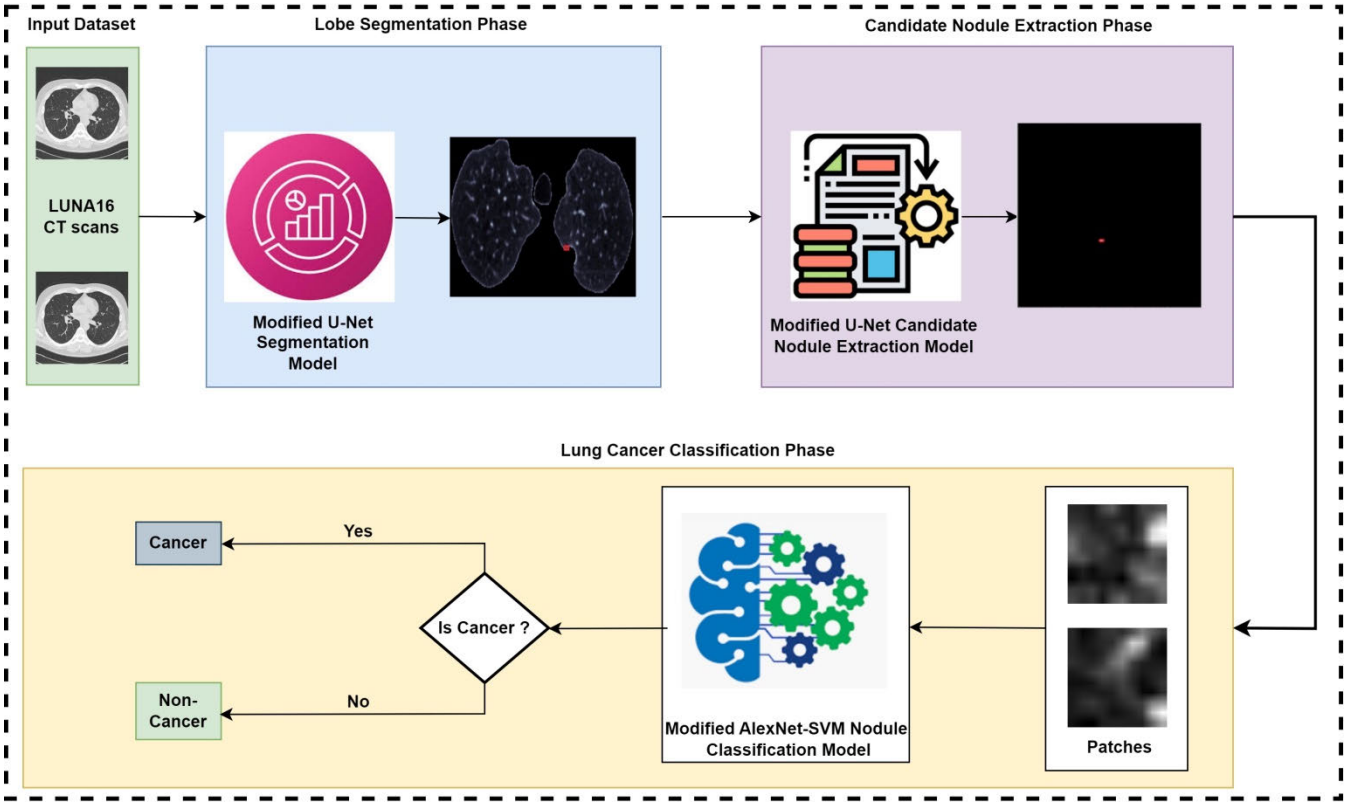

FIGURE 1. Proposed lung cancer classification using modified U-Net-based lobe segmentation and nodule detection model.

improve accuracy [35], [40], [44], [47], [48], [51] lack of transparency [15].

The core contribution of this research is as following:

- The main objective of this research is to provide the lung cancer classification method using modified U-Net based lobe segmentation and nodule detection.
- To enhance the effectiveness of the segmentation model, we have implemented modified U-Net architecture for lobe segmentation and ensure that lobe-segmentation model training, validation and testing are brought out efficiently.
- The performance of the suggested candidate nodule extraction model has been used modified U-Net architecture for the detection of nodule and it provides better results and investigated using various performance statistical indicators.
- Finally, lung cancer classification model using AlexNet and Support vector machine (SVM) for the classification is proposed and it classifies the lung nodule into cancer and non-cancer. The proposed model achieves better results for accurate and effective lung cancer classification and treatment.

The rest of the paper is structured as follows; Section II covers the literature review, Section III illustrates the proposed methodology, and the results and discussion wrap up in Section IV. Section V concludes with a conclusion and Section VI describes limitation and future work.

III. PROPOSED METHODOLOGY

Lung cancer disease is referred to as the most lethal disease among all other cancers. Detection of lung cancer at an early stage plays a major role in the successful treatment and increases the survival rate. Various methods are used to detect lung cancer such as CT, biopsy, blood test, and X-ray. Pulmonary nodule detection is a challenging task because of the various size, shapes, locations of nodules, and densities. Computational intelligence techniques have been utilized to detect lung cancer timely.

In this section, we propose lung cancer classification using modified U-Net based lobe segmentation and nodule detection model as demonstrated in Figure 1.

The model consists of three phases: Lobe segmentation, candidate nodule extraction, and lung cancer classification. In the lobe segmentation phase, modified U-Net architecture is used to segment the input CT scans, and lobes are derived as output. Whereas the next candidate nodule extraction phase uses predicted lobes as input and modified U-Net based model is applied for the extraction of the candidate nodule. Furthermore, modified AlexNet-SVM based model is applied on patches of candidate nodules in the third phase and classifies candidate nodules as non-cancer and cancer.

A. LOBE SEGMENTATION PHASE

Lobe segmentation is the first phase of the lung cancer classification using modified U-Net based lobe segmentation and

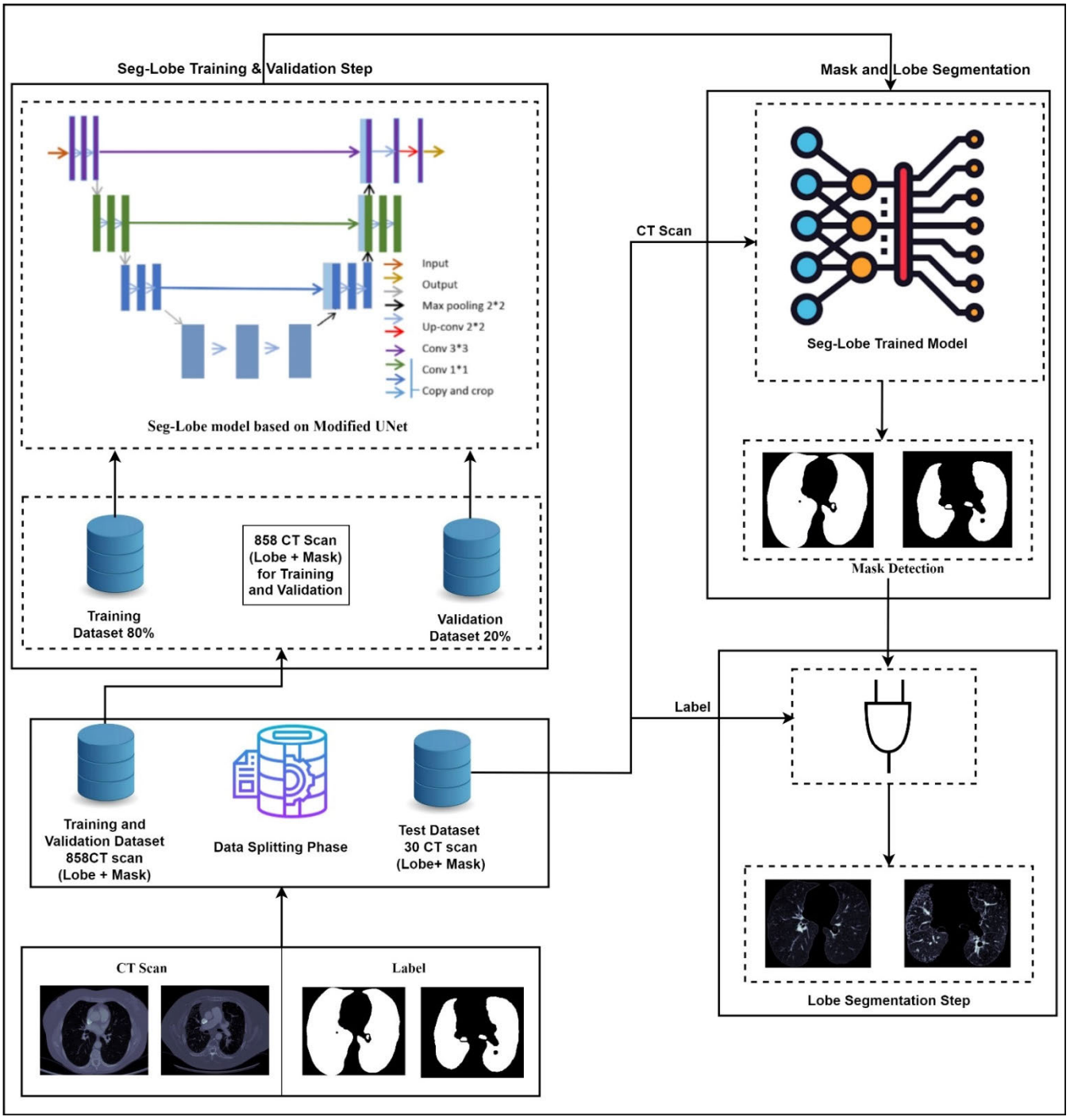

FIGURE 2. Proposed modified U-Net architecture for lobe segmentation.

nodule detection model as shown in Figure 2. In this phase, modified U-Net architecture is applied to the segment lobe from CT scan images. The segmentation phase consists of two steps: seg-lobe training and validation step and lobe segmentation step. In the seg-lobe step, modified U-Net based model trained and validated on LUNA16 CT scans dataset.

In the second step, the modified U-Net based model for lobe segmentation predicts the mask from the test CT scans dataset and by using the predicted mask, the lobe is extracted. In this phase, the LUNA16 dataset consists of CT scans with labels that are used as input to the proposed method for segmentation. The lung cancer dataset consists of 888 CT scans which is divided into 589 for cancer and 299 indicates non-cancer. In this research a total number of 30 cancer CT scans are separated for testing of the proposed method by using random selection technique. A total number of 858 cancer and non-cancer CT scans is separated for training and validation, and it is further divided into 80% (686 CT scans)

for training and 20% (172 CT scans) for validation of the model for the lobe segmentation. The model is trained on the 686 CT scans training dataset. After the training of the seg-lobe model, it is validated on 172 CT scans. A total number of 30 CT scans are provided to the seg-lobe model for testing for the segmentation of CT scans. The seg-lobe model predicts the masks from the testing 30 CT scans. Finally, the lobe from slices of 30 CT scans is segmented using the predicted mask of slices. U-Net architecture was designed by Ronneberger et al. [33] for medical image segmentation in 2015.

U-Net architecture consisted of three main blocks, encoder, decoder, and skip connection as shown in Figure 3.

The Encoder block receives the image as input and then extracts useful features from an image using multiple convolutional layers. Decoder block U-Net architecture is a combination of several convolutional layers and transposed convolutional layers. The convolutional layer represents in Eq. (1) and transposed convolutional layer represents in Eq. (2).

$$\varphi = f\left(\omega * \alpha + \flat\right) \tag{1}$$

where α denotes the input, ω shows the layer's weight and $\flat$ represents the bias parameter and expresses the activation function.

$$\varphi = f\left(\omega' * \alpha + \flat\right) \tag{2}$$

where α denotes the input, ω' shows the layer's transposed weight matrix and $\flat$ represents the bias parameter and expresses the activation function.

U-Net architecture also comprises concatenation operations. Where feature maps from contracting combine with feature maps from the expanding paths. The mathematical representation of concatenation operations is shown in Eq. (3).

$$\varphi = concatenate\left(\alpha 1 + \alpha 2\right) \tag{3}$$

where $\alpha 1$ and $\alpha 2$ represent the feature maps.

In the first phase of the lung cancer classification using modified U-Net based lobe segmentation and nodule detection method, the image input dimension is 512 × 512 × 1 followed by two convolutional layers. Convolutional operations are performed on two convolutional layers with 8 filter size, ReLU activation function is used 3 × 3 kernel size, and the same padding, the output 512 × 512 × 8 is denoted by C1.

The convolutional layer is the primary component of CNN architecture where important features are extracted from the input data. For this, convolutional operations are performed and denoted by *, the output of the convolutional operations is called a features map. The convolutional operations are represented in Eq. (4).

$$(m * n)(p) = \int m(u)\, n(p - u)\, du \tag{4}$$

where the input matrix (image) is denoted m, n is the filter or kernel, and convolutional operation is represented as *.

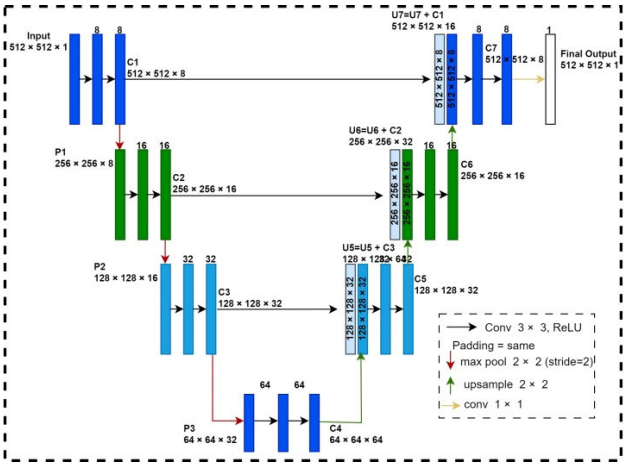

FIGURE 3. Proposed modified U-Net architecture for lobe segmentation.

The output of the convolution is called a feature map and is represented by (m*n)(p) and forwarded to a nonlinear activation function.

Various nonlinear activation functions such as ReLU, Softmax, Hyperbolic tangent (Tanh), and Sigmoid are applied to remove linearity values. In this model, the nonlinear ReLU activation function is applied and mathematically represented in Eq. (5).

$$f(y) = \max(0, y) \tag{5}$$

Kernel initializer such as 'he_normal' is applied to initialize the weights of a layer and prevent the vanishing gradients problem. The initializer 'he_normal' is mostly used while the ReLU activation function is applied in this research.

Next, the pooling layer is applied to reduce the spatial dimensionality of the feature maps however, it retains the important information. Various types of pooling layers such as min pooling, max pooling, sum pooling, and average pooling can be applied to reduce the dimensionality of the feature map. In the proposed model, max pooling is applied on the feature map, and it is represented in the Eq. (6).

$$z[g][h] = \max\left(y[g : g + j][h : h + j]\right) \tag{6}$$

where y represents the input feature map, z denotes the output feature map, k is pool size, and g,h are the indexes of the output feature map. Max operation is performed a j × j window of the input feature map and the maximum value is assigned to the corresponding location in the output feature map. Next, the sigmoid activation function applies and 512 × 512 × 8 is forwarded to the sigmoid activation function represented in Eq. (7).

$$sigmoid\left(C7\right) = \frac{1}{\left(1 + e^{c7}\right)} \tag{7}$$

where C7 is the input to the sigmoid activation function.

A deep learning-based model requires computational resources and extensive time for training. Various optimizers such as gradient descent, stochastic gradient descent (SGD), Adagrad, root mean square propagation (RMSprop), and

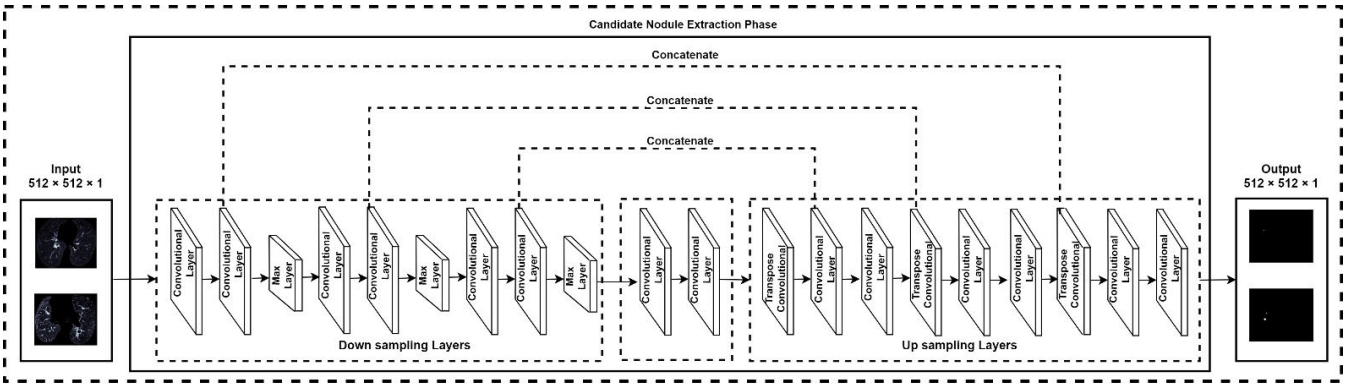

FIGURE 4. Proposed modified U-Net architecture for candidate nodule extraction.

adaptive moment estimation (Adam) can be utilized to optimize model performance and reduce the error rate. Adam's method uses an adaptive learning rate to compute parameters at each iteration and shows Eq. (8) to Eq. (11).

$$g_t = \Upsilon_1 \times g_{t-1} - (1 - \beta_1) \times h_t \tag{8}$$

$$s_t = \Upsilon_2 \times s_{t-1} - (1 - \beta_2) \times h_t \tag{9}$$

$$\Delta j_t = -h_t \frac{g_t}{\sqrt{m_t + \varepsilon}} * \times h_t \tag{10}$$

$$j_{t+1} = j_t + \eta \times \Delta j_t \tag{11}$$

where η represents the initial learning rate, denotes exponential gradients average along with, shows gradient at time t along, express the exponential average of squares of gradients along, and shows hyperparameters. In this model, Adam optimizer is applied to increase the efficiency and decrease the error rate of the proposed model. Finally, 1 × 1 convolutional operation is performed on C9 and 512 × 512 × 1 as the final output is achieved for the segmentation of Lobes.

B. CANDIDATE NODULE EXTRACTION PHASE

The second phase of the lung cancer classification using modified u-net based lobe segmentation and nodule detection model is called candidate nodule extraction is shown in Figure 4. In this research, a total of 888 CT scans in which 589 CT scans for cancerous and 299 CT scans for non-cancerous.

This phase uses 589 cancer CT scan for training, validation, and testing of the modified U-Net architecture for the candidate nodule extraction model. We use the slices from 30 cancer CT scans for testing the model. Slices from 559 cancer CT scan is further divided into 80% (slices from 447 CT scan) for training and 20% (slices from 112 CT scan) for validation of the candidate nodule extraction model. This model is trained on the slices obtained from 447 cancer CT scans training dataset. When the training of the candidate nodule extraction model, the model is validated on slices obtained from 112 cancer CT scans.

Furthermore, in the testing step, slices from 30 CT scans are used for testing the candidate nodule extraction model. The modified U-Net architecture for the candidate nodule extraction model predicts the candidate nodule mask from the lobes of slices of testing 30 cancer CT scans. Finally, the model predicts the candidate nodule by using the predicted mask and label.

C. LUNG CANCER CLASSIFICATION PHASE

Finally, the last phase of the lung cancer classification using modified U-Net based lobe segmentation and nodule detection model classifies cancer or non-cancer using patches from the candidate nodules.

In this research, patch size 48 × 48 is selected that based on nodule and pixel size to train, validate, and test the modified AlexNet-SVM architecture for Lung Cancer Classification. A total number of 17006 patches are obtained from slices of 858 cancer and non-cancer CT scan. It is further divided into 80% (13605) patches for training and 20% (3401) patches for validation of the model. Patches obtained from slices of 30 CT scan is used to test the model and it predicts lung cancer into non-cancer and cancer. Modified AlexNet-SVM architecture for lung cancer classification consists of lung cancer classification training and validation phase and lung cancer classification phase is shown in Figure 5.

In the lung cancer classification training and validation phase, modified AlexNet-SVM architecture model is trained and validated on 48 × 48 patch size. Modified AlexNet architecture extracted features from input patches to obtain important information. Stochastic gradient descent (SGD) optimizer is used with hyperparameters such as 200 epochs, 50 batch size, and 0.0001 learning rate. The modified AlexNet architecture comprises eight convolutional and three max pooling layers. The convolutional layer is responsible for extracting valuable features from patches and pooling layer and which is used to reduce the size of the feature map but keeps the important information. In this research, max pooling layer is used on the feature map. After the max pooling layer, the feature map matrix is transformed into a single long vector, and it is called flattening.

The modified AlexNet architecture takes input 48 × 48 × 1 grayscale patch size as demonstrated in Figure 6. The first three convolutional layers are used 32 filters along with 3 × 3 filter size, the same padding, and ReLU AF

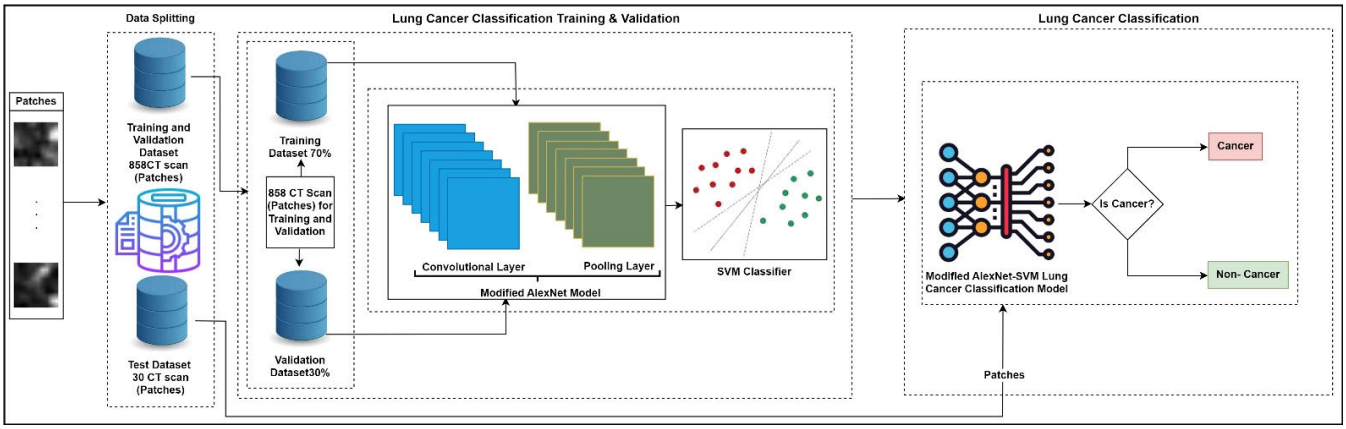

FIGURE 5. Proposed modified AlexNet architecture for classification of lung cancer patches.

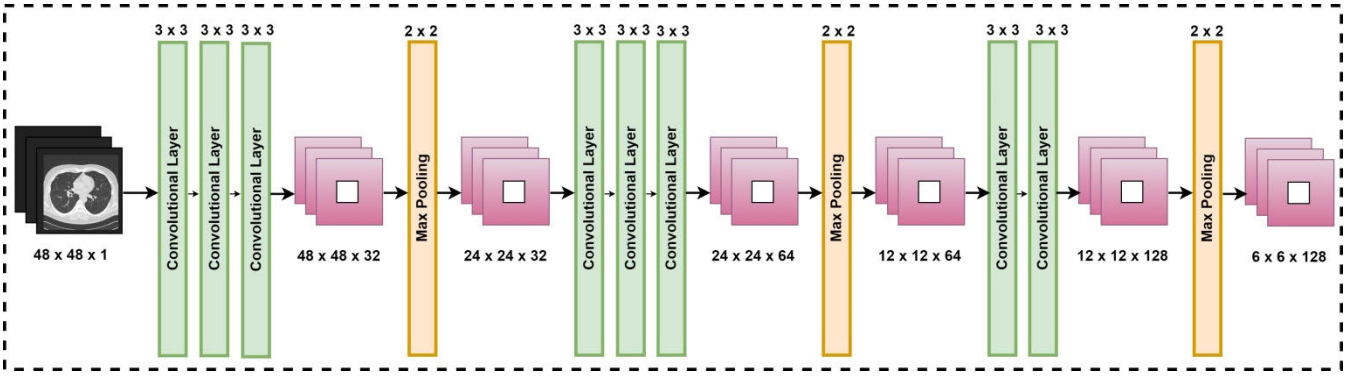

FIGURE 6. Proposed modified AlexNet architecture for classification of lung cancer patches.

is applied to remove non-linearity from the feature map. Next, the max pooling layer is used 2×2 filter size, stride 2 and resulting patch size reduces and dimension of patches become $24 \times 24 \times 32$.

The sigmoid activation function produces class score from the output of a fully connected layer. Finally, SVM is utilized to classify lung cancer into cancer and non-cancer. Afterward, training and validation of the modified AlexNet-SVM model, the patches from the 30 testing CT scans are forwarded to the model to evaluate the performance of the modified AlexNet-SVM architecture for lung cancer classification and classify patches into cancer and non-cancer.

IV. SIMULATION RESULTS

Generally, digital imaging and communications in medicine (DICOM) files are used to store CT scan images. The DICOM file comprises the CT image along with image information in the DICOM header and raw data related to the CT image. The slices of CT scan have instance numbers which are also mentioned in the DICOM header. The lung cancer classification uses modified U-Net based lobe segmentation, and the nodule detection method takes LUNA16 CT scans dataset as input for the detection of lung cancer using computational intelligence techniques. LUNA16 dataset is stored in the form of MetaImage (mhd/raw) format. LUNA16 dataset contains 888 CT scans which are further divided into 589 cancer CT scans and 299 non-cancer CT scans.

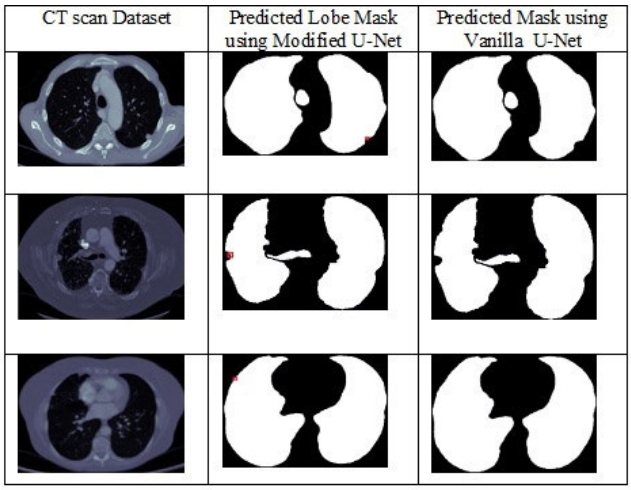

FIGURE 7. Lobe mask prediction using modified U-Net architecture and vanilla U-Net architecture.

A total number of slices from 30 CT scans are separated from cancer CT scan for testing of the proposed methodology. In the lobe-segmentation phase, the remaining slices from 858 CT scans have been used for training and validation purposes while slices from 30 CT scans have been used for testing the proposed model. Next, slices from 589 cancer CT scans are utilized to train, validate, and test the proposed methodology. Slices from 559 CT scans have been utilized for training and validation and the remaining slices

TABLE 2. Comparison analysis of candidate nodule extraction using modified U-Net architecture and vanilla U-Net model with existing state-of-the-art methods.

Model	Dataset	Dice	Sensitivity	Precision
Ali et al. [12]	LIDC-IDRI	81.1%	82%	-
SKV-Net [37]	LIDC-IDRI	0.796	0.789	-
Tyagi et al. [20]	LUNA16	80.74	85.46	80.56
Lu et al. [38]	LIDC-IDRI	0.7442	0.7254	0.7551
Liang et al. [36]	LIDC-IDRI	86.89%	85.11%	89.47%
Vanilla U-Net	LUNA16	78.57%	64.71%	74.83%
Proposed Modified Candidate Nodule model	**LUNA16**	**88.31%**	**85.53%**	**91.28%**

TABLE 3. Confusion matrix of modified AlexNet-SVM classification model (Training).

No. of Patches = 13604	Output Class	
Input Class	Non-Cancer	Cancer
Non-Cancer (6802)	6715	87
Cancer (6802)	95	6707

from 30 cancer CT scans are separated for testing purposes. Finally, a total number of 17006 patches are obtained from slices of 858 cancer and non-cancer CT scans have been utilized to train and validate the proposed model the trained model predicts cancer and non-cancer patches by using slices from 30 cancer CT scans which are separated for testing purposes.

The performance of the proposed methodology is measured using various statistical metrics. Various performance metrics, including Dice, IoU, sensitivity, and precision have been applied to assess the performance of the proposed model. Mostly, Dice and IoU statistical metrics are applied for segmentation techniques. The Dice metric evaluates the connection between the segmented output and ground truth.

The IoU calculates the area of overlap between the ground truth and predicted segmentation based on the union of the outputs of the ground truth and predicted segmentation. Sensitivity and precision metrics are also applied to assess the robustness of the proposed model. In the lobe segmentation step, the original size 512 × 512 of the CT images are utilized in the proposed model. Dice, IoU, sensitivity, and precision are used to evaluate the performance of the Lobe segmentation model. Segmentation lobe step, U-Net based modified architecture has been applied to segment the lobe.

A. RESULTS OF LOBE SEGMENTATION PHASE

In the Lobe segmentation phase, modified U-Net architecture for the lobe segmentation model segments the input CT scan images into the lobe. The modified U-Net architecture for lobe segmentation and Vanilla U-Net predicts mask from the input CT scan dataset and results are shown in Figure 7. The

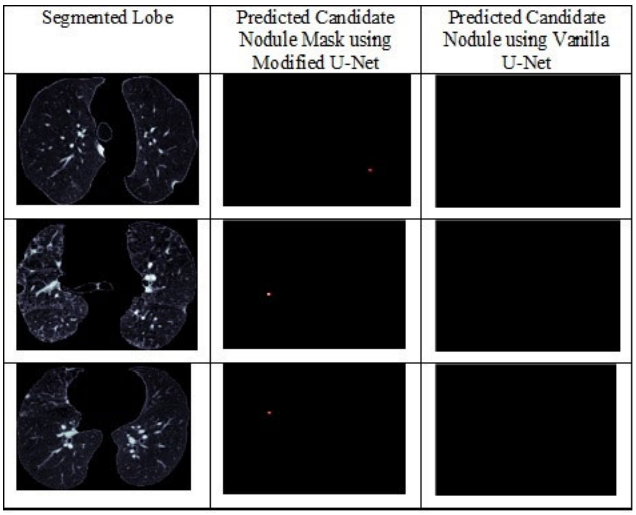

FIGURE 8. Candidate nodule extraction using modified U-Net architecture and vanilla U-Net.

TABLE 4. Confusion matrix of modified AlexNet-SVM classification model (Testing).

No. of Patches = 1188	Output Class	
Input Class	Non-Cancer	Cancer
Non-Cancer (594)	579	15
Cancer (594)	9	585

lobe segmentation phase consists of two steps, one is the Seg-Lob training and validation step and the second is called Lobe segmentation step. In the first step, Seg-Lobe based on modified U-Net architecture consists of three encoders, three decoders, and three skip connections. The seg-Lobe model is used to train 80% of the dataset and after the training step, the Seg-Lobe model validates on 20% of the dataset of the CT scan images. In the next step, CT scans test dataset is provided to Seg-Lobe trained model to predict the mask of CT scan images. Then label of the test dataset is provided to segment the lobe and the lobe is extracted by using the predicted mask.

TABLE 5. Comparison analysis of lung cancer classification by using AlexNet-SVM model.

Model	Dataset	Accuracy (%)	Sensitivity (%)	Specificity (%)	Precision	F1-score
Halder et al. [15]	LIDC-IDRI	96.10	96.85	95.17	-	-
Fu et al. [35]	LIDC-IDRI	94.7	96.2	82.9	97.8	-
He et al. [38]	LIDC-IDRI	9.873	0.862	0.885	-	-
Huidrom et al. [39]	LUNA16	95.5	95.8	95.3	-	-
Suresh et al. [40]	LIDC-IDRI	93.9	93.4	93	-	-
Bhaskar et al. [44]	LUNA16	93.2	71.2	98.2	89.3	-
Han et al. [45]	LUNA16	0.911	0.969	-	-	-
Bruntha et al. [46]	LIDC-IDRC	97.53	98.62	96.88	95.04	96.79
Al-Shabi et al. [47]	LIDC-IDRI	94.11	94.09	-	94.54	93.81
Huang et al. [48]	LIDC-IDRI	92.13	87.16	-	94.16	89.93
Dodia et al. [50]	LUNA16	94.87	95.12	94.62	94.53	0.9483
Lye et al.[51]	LIDC-IDRI	92.19	92.10	91.50	-	-
Proposed Modified AlexNet-SVM model	**LUNA16**	**97.98**	**98.84**	**97.47**	**97.5**	**97.99**

The outcomes of performance indicators including Dice, IoU, sensitivity, and precision are 90.32%, 82.35%, 87.5% and 93.33% respectively obtains by modified U-Net architecture for lobe mask prediction and Vanilla U-Net achieves 83.40% of Dice, 72.35% of IoU, 82.55% of sensitivity and 85.42% of precision.

B. RESULTS OF CANDIDATE NODULE EXTRACTION PHASE

The next phase of lung cancer classification using modified U-Net based lobe segmentation and nodule detection method is candidate nodule extraction from the input segmented lobe. The modified U-Net architecture for candidate nodule extraction and Vanilla U-Net predicts candidate nodule mask from the segmented lobe and results are shown in Figure 8.

The candidate nodule extraction phase consists of two steps, one is the candidate nodule extraction training and validation phase where proposed model is trained and validated. In the second step is called mask and candidate nodule extraction phase. Candidate nodule extraction consists of three encoders, three decoders and three skip connections. The candidate nodule extraction model is used to train 80% of the dataset and after the training step, the candidate nodule extraction model validates from 20% of the dataset of the CT scan images. Candidate nodule extraction model using modified U-Net architecture is trained and validated on training and validating datasets.

In the next step, the segmented lobe test dataset is provided to the candidate nodule extraction trained model to predict the mask and then the label of the test dataset is provided to extract the nodule, and the nodule is extracted by using the predicted mask. Comparison analysis for candidate nodule extraction using modified U-Net architecture, Vanilla U-Net and existing state-of-the-art approaches illustrated in Table 2.

C. RESULTS OF LUNG CANCER CLASSIFICATION PHASE

The last phase of lung cancer classification using modified U-Net based lobe segmentation and nodule detection method consists of lung nodule classification. The lung nodule classification phase comprises two steps. The first step is called training and validation of the lung cancer classification phase and the second step is called the lung cancer classification phase. In the first step, the patches from 858 CT scans are used and divided into 80% for training and 20% for validation purposes. Modified AlexNet architecture consists of eight convolutional layers and three max-pooling layers followed by two fully connected layers and the SVM classifier has been applied to the classification of lung cancer. When the classification model is trained on 80% of patches and validated on 20% of patches. The trained model is tested on patches obtained from 30 CT scans. A confusion matrix has been employed to evaluate the performance of modified AlexNet-SVM model to classify the lung nodules. A total number of 13604 patches from 858 cancer and non-cancer CT scans are obtained to train modified AlexNet-SVM model shown in Table 3.

A total number of 13604 sample patches are divided into two groups named cancer and non-cancer. In the non-cancer group, a total number of 6802 non-cancer patches are used to train the AlexNet-SVM model and it correctly predicts 6715 sample patches as non-cancer and predicts wrongly 87 sample patches. In the cancer group, a total number of 6802 sample patches are used for the prediction of cancer, the modified AlexNet-SVM model wrongly predicts 95 sample patches as non-cancer and correctly predicts 6707 sample patches as cancer.

Confusion matrix of modified AlexNet-SVM classification model for testing is shown in Table 4.

A total number of 1188 patches are obtained to test modified AlexNet-SVM. Furthermore, a total number of 1188 sample patches are divided into two groups named cancer and non-cancer. In the non-cancer group, a total number of 594 patches are used to test the performance of the modified AlexNet-SVM model and it correctly predicts 579 sample patches as non-cancer and wrongly predicts 15 sample patches. In the cancer group, a total number of 594 sample patches are used for the prediction of cancer, the modified AlexNet-SVM model wrongly predicts 9 sample patches as non-cancer and correctly predicts 585 sample patches as cancer.

The various statistical metrics for evaluation such as accuracy, miss rate, sensitivity, specificity, precision, and

F1 are used to test the performance of the modified AlexNet-SVM model as presented in Table 5.

Other parameters have also been calculated for the performance of the proposed model such as a Negative predictive value of 98.03%, false. negative rate of 2.14%, false positive rate of 2.27%, false discovery rate of 2.47%, and false omission rate of 1.96%.

V. CONCLUSION

This research presents efficient and effective methods for lobe segmentation, candidate nodule extraction, and lung cancer classification which improved the accuracy. The model uses modified U-Net architecture for lobe segmentation and candidate nodule extraction. Furthermore, modified AlexNet-SVM applies to the classification of pulmonary nodules. The modified AlexNet-SVM based model comprises eight convolutional, three pooling, two fully connected layers, and an SVM algorithm that is used to classify lung cancer.

The experimental outcomes for the segmentation lobe using modified U-Net model are 90.32% of Dice, 82.35% of IoU, 87.5% of Sensitivity, and 93.33% of precision, whereas Vanilla U-Net achieves 83.40% of Dice, 72.35% of IoU, 82.55% of sensitivity and 85.42% of precision. Next, modified U-Net candidate nodule extraction model shows results Dice 87.42%, 77.65% of IoU, 92.96% of sensitivity, and 82.5% of precision whereas Vanilla U-Net achieves 78.57% of Dice, 64.71% of sensitivity, 74.83% of precision and 82.71% of IoU for candidate nodule extraction. Finally, the nodule classification phase of the proposed model shows 97.98% of accuracy, 98.84% of sensitivity, 97.47% of specificity, 97.53% of precision, and 97.70% of F1. The experimental results of lung cancer classification using modified U-Net based lobe segmentation and nodule detection model have shown outstanding performance.

VI. LIMITATION AND FUTURE WORK

Lung cancer classification using modified U-Net based lobe segmentation and nodule detection model segments candidate nodules and classifies lung cancer into non-cancer and cancer. The model based on modified U-Net architecture to segment lobe and candidate nodule and modified AlexNet architecture with SVM is applied to classify the lung nodules. The current research has some limitations, for example, it used the LUNA16 dataset to train, validate, and test purposes. The other publicly available lung cancer datasets can be implemented to test the performance of the Lung cancer classification using modified U-Net based lobe segmentation and nodule detection model.

REFERENCES

[1] R. L. Siegel, K. D. Miller, N. S. Wagle, and A. Jemal, "Cancer statistics, 2023," *CA, Cancer J. Clinicians*, vol. 73, no. 1, pp. 17–48, Jan. 2023, doi: 10.3322/caac.21763.

[2] G. Zhang, Z. Yang, L. Gong, S. Jiang, and L. Wang, "Classification of benign and malignant lung nodules from CT images based on hybrid features," *Phys. Med. Biol.*, vol. 64, no. 12, pp. 1–12, 2019, doi: 10.1088/1361-6560/ab2544.

[3] M. Mubashar, H. Ali, C. Grönlund, and S. Azmat, "R2U++: A multiscale recurrent residual U-Net with dense skip connections for medical image segmentation," *Neural Comput. Appl.*, vol. 34, no. 20, pp. 17723–17739, Oct. 2022, doi: 10.1007/s00521-022-07419-7.

[4] J. Soltani-Nabipour, A. Khorshidi, and B. Noorian, "Lung tumor segmentation using improved region growing algorithm," *Nucl. Eng. Technol.*, vol. 52, no. 10, pp. 2313–2319, Oct. 2020, doi: 10.1016/j.net.2020.03.011.

[5] M. Wang and D. Li, "An automatic segmentation method for lung tumor based on improved region growing algorithm," *Diagnostics*, vol. 12, no. 12, p. 2971, Nov. 2022.

[6] R. Bellotti, F. De Carlo, G. Gargano, S. Tangaro, D. Cascio, E. Catanzariti, P. Cerello, S. C. Cheran, P. Delogu, I. De Mitri, C. Fulcheri, D. Grosso, A. Retico, S. Squarcia, E. Tommasi, and B. Golosio, "A CAD system for nodule detection in low-dose lung CTs based on region growing and a new active contour model," *Med. Phys.*, vol. 34, no. 12, pp. 4901–4910, Nov. 2007, doi: 10.1118/1.2804720.

[7] J. Zhao, M. Dang, Z. Chen, and L. Wan, "DSU-Net: Distraction-sensitive U-Net for 3D lung tumor segmentation," *Eng. Appl. Artif. Intell.*, vol. 109, Mar. 2022, Art. no. 104649, doi: 10.1016/j.engappai.2021.104649.

[8] T. Meraj, H. T. Rauf, S. Zahoor, A. Hassan, M. I. Lali, L. Ali, S. A. C. Bukhari, and U. Shoaib, "Lung nodules detection using semantic segmentation and classification with optimal features," *Neural Comput. Appl.*, vol. 33, no. 17, pp. 10737–10750, Sep. 2021, doi: 10.1007/s00521-020-04870-2.

[9] N. S. Rani, "Extraction of gliomas from 3D MRI images using convolution kernel processing and adaptive thresholding," *Proc. Comput. Sci.*, vol. 167, pp. 273–284, Jan. 2020, doi: 10.1016/j.procs.2020.03.221.

[10] Y. R. Baby and V. K. R. Sumathy, "Kernel-based Bayesian clustering of computed tomography images for lung nodule segmentation," *IET Image Process.*, vol. 14, no. 5, pp. 890–900, Apr. 2020, doi: 10.1049/iet-ipr.2018.5748.

[11] F. Calabrese, F. Pezzuto, F. Lunardi, F. Fortarezza, S.-E. Tzorakoleftheraki, M. V. Resi, M. Tiné, G. Pasello, and P. Hofman, "Morphologic-molecular transformation of oncogene addicted non-small cell lung cancer," *Int. J. Mol. Sci.*, vol. 23, no. 8, p. 4164, Apr. 2022, doi: 10.3390/ijms23084164.

[12] Z. Ali, A. Irtaza, and M. Maqsood, "An efficient U-Net framework for lung nodule detection using densely connected dilated convolutions," *J. Supercomput.*, vol. 78, no. 2, pp. 1602–1623, Feb. 2022, doi: 10.1007/s11227-021-03845-x.

[13] Y. Lan, N. Xu, X. Ma, and X. Jia, "Segmentation of pulmonary nodules in lung CT images based on active contour model," in *Proc. 14th Int. Conf. Intell. Hum.-Mach. Syst. Cybern. (IHMSC)*, Aug. 2022, pp. 132–135, doi: 10.1109/IHMSC55436.2022.00039.

[14] S. Dlamini, Y. H. Chen, and C. F. Jeffrey Kuo, "Complete fully automatic detection, segmentation and 3D reconstruction of tumor, volume for non-small cell lung cancer using YOLOv4 and region-based active contour model," *Expert Syst. Appl.*, vol. 212, pp. 1–9, Feb. 2023, doi: 10.1016/j.eswa.2022.118661.

[15] A. Halder, S. Chatterjee, and D. Dey, "Adaptive morphology aided 2-pathway convolutional neural network for lung nodule classification," *Biomed. Signal Process. Control*, vol. 72, Feb. 2022, Art. no. 103347, doi: 10.1016/j.bspc.2021.103347.

[16] J. Jiang, J. Mei, S. Jiang, J. Zhang, L. Wang, J. Yuan, S. Yi, Y. Ma, and Y. Liu, "Lung cancer shapes commensal bacteria via exosome-like nanoparticles," *Nano Today*, vol. 44, Jun. 2022, Art. no. 101451, doi: 10.1016/j.nantod.2022.101451.

[17] L. Rinaldi, F. Pezzotta, T. Santaniello, P. De Marco, L. Bianchini, D. Origgi, M. Cremonesi, P. Milani, M. Mariani, and F. Botta, "HeLLePhant: A phantom mimicking non-small cell lung cancer for texture analysis in CT images," *Phys. Medica*, vol. 97, pp. 13–24, May 2022, doi: 10.1016/j.ejmp.2022.03.010.

[18] G. Zhang, Z. Yang, and S. Jiang, "Automatic lung tumor segmentation from CT images using improved 3D densely connected UNet," *Med. Biol. Eng. Comput.*, vol. 60, no. 11, pp. 3311–3323, Nov. 2022, doi: 10.1007/s11517-022-02667-0.

[19] M. Kanipriya, C. Hemalatha, N. Sridevi, S. R. SriVidhya, and S. L. J. Shabu, "An improved capuchin search algorithm optimized hybrid CNN-LSTM architecture for malignant lung nodule detection," *Biomed. Signal Process. Control*, vol. 78, pp. 1–39, Sep. 2022, doi: 10.1016/j.bspc.2022.103973.

[20] S. Tyagi and S. N. Talbar, "CSE-GAN: A 3D conditional generative adversarial network with concurrent squeeze-and-excitation blocks for lung nodule segmentation," *Comput. Biol. Med.*, vol. 147, Aug. 2022, Art. no. 105781, doi: 10.1016/j.compbiomed.2022.105781.

[21] Y. Ni, Z. Xie, D. Zheng, Y. Yang, and W. Wang, "Two-stage multitask U-Net construction for pulmonary nodule segmentation and malignancy risk prediction," *Quant. Imag. Med. Surgery*, vol. 12, no. 1, pp. 292–309, Jan. 2022, doi: 10.21037/qims-21-19.

[22] H. Cao, H. Liu, E. Song, C.-C. Hung, G. Ma, X. Xu, R. Jin, and J. Lu, "Dual-branch residual network for lung nodule segmentation," *Appl. Soft Comput. J.*, vol. 86, pp. 1–8, Jan. 2020, doi: 10.1016/j.asoc.2019.105934.

[23] J. Sun, W. Chen, L. Zhang, and X. Yan, "Research on lung tumor cell segmentation method based on improved UNet algorithm," *Sci. Program.*, vol. 2022, pp. 1–8, Jul. 2022, doi: 10.1155/2022/6357123.

[24] J. Yang, B. Wu, L. Li, P. Cao, and O. Zaiane, "MSDS-UNet: A multi-scale deeply supervised 3D U-Net for automatic segmentation of lung tumor in CT," *Comput. Med. Imag. Graph.*, vol. 92, pp. 1–10, Sep. 2021, doi: 10.1016/j.compmedimag.2021.101957.

[25] Z. Zhou, F. Gou, Y. Tan, and J. Wu, "A cascaded multi-stage framework for automatic detection and segmentation of pulmonary nodules in developing countries," *IEEE J. Biomed. Health Informat.*, vol. 26, no. 11, pp. 5619–5630, Nov. 2022, doi: 10.1109/JBHI.2022.3198509.

[26] S. Wang, A. Jiang, X. Li, Y. Qiu, M. Li, and F. Li, "DPBET: A dual-path lung nodules segmentation model based on boundary enhancement and hybrid transformer," *Comput. Biol. Med.*, vol. 151, Dec. 2022, Art. no. 106330, doi: 10.1016/j.compbiomed.2022.106330.

[27] S. Luo, J. Zhang, N. Xiao, Y. Qiang, K. Li, J. Zhao, L. Meng, and P. Song, "DAS-Net: A lung nodule segmentation method based on adaptive dual-branch attention and shadow mapping," *Int. J. Speech Technol.*, vol. 52, no. 13, pp. 15617–15631, Oct. 2022, doi: 10.1007/s10489-021-03038-2.

[28] P. M. Bruntha, S. I. A. Pandian, K. M. Sagayam, S. Bandopadhyay, M. Pomplun, and H. Dang, "Lung_PAYNet: A pyramidal attention based deep learning network for lung nodule segmentation," *Sci. Rep.*, vol. 12, no. 1, pp. 1–11, Nov. 2022, doi: 10.1038/s41598-022-24900-4.

[29] I. Naseer, T. Masood, S. Akram, A. Jaffar, M. Rashid, and M. A. Iqbal, "Lung cancer detection using modified AlexNet architecture and support vector machine," *Comput., Mater. Continua*, vol. 74, no. 1, pp. 2039–2054, 2023, doi: 10.32604/cmc.2023.032927.

[30] Y. Cao, L. Liu, X. Chen, Z. Man, Q. Lin, X. Zeng, and X. Huang, "Segmentation of lung cancer-caused metastatic lesions in bone scan images using self-defined model with deep supervision," *Biomed. Signal Process. Control*, vol. 79, Jan. 2023, Art. no. 104068, doi: 10.1016/j.bspc.2022.104068.

[31] J. Park, S. K. Kang, D. Hwang, H. Choi, S. Ha, J. M. Seo, J. S. Eo, and J. S. Lee, "Automatic lung cancer segmentation in [18F]FDG PET/CT using a two-stage deep learning approach," *Nucl. Med. Mol. Imag.*, vol. 57, no. 2, pp. 86–93, Apr. 2023, doi: 10.1007/s13139-022-00745-7.

[32] J. Long, E. Shelhamer, and T. Darrell, "Fully convolutional networks for semantic segmentation," in *Proc. IEEE Conf. Comput. Vis. Pattern Recognit. (CVPR)*, Jun. 2015, pp. 3431–3440.

[33] O. Ronneberger, P. Fischer, and T. Brox, "U-Net: Convolutional networks for biomedical image segmentation," in *Proc. Int. Conf. Med. Image Comput. Comput.-Assist. Intervent.*, 2015, pp. 234–241.

[34] G. Singadkar, A. Mahajan, M. Thakur, and S. Talbar, "Deep deconvolutional residual network based automatic lung nodule segmentation," *J. Digit. Imag.*, vol. 33, no. 3, pp. 678–684, Jun. 2020.

[35] X. Fu, L. Bi, A. Kumar, M. Fulham, and J. Kim, "An attention-enhanced cross-task network to analyse lung nodule attributes in CT images," *Pattern Recognit.*, vol. 126, no. 3, pp. 1–32, 2022.

[36] G. Liang, Z. Diao, and H. Jiang, "Uncertainty analysis based attention network for lung nodule segmentation from CT images," in *Proc. 6th Int. Conf. Virtual Augmented Reality Simulations*, Mar. 2022, pp. 50–55, doi: 10.1145/3546607.3546615.

[37] Z. Wang, J. Men, and F. Zhang, "Improved V-Net lung nodule segmentation method based on selective kernel," *Signal, Image Video Process.*, vol. 17, no. 5, pp. 1763–1774, Jul. 2023, doi: 10.1007/s11760-022-02387-w.

[38] W. He and B. Li, "Knowledge-based systems an ISHAP-based interpretation-model-guided classification method for malignant pulmonary nodule," *Knowl. Base Syst.*, vol. 237, no. 2, pp. 1–44, 2022.

[39] R. Huidrom, Y. J. Chanu, and K. M. Singh, "Neuro-evolutional based computer aided detection system on computed tomography for the early detection of lung cancer," *Multimedia Tools Appl.*, vol. 81, no. 22, pp. 32661–32673, Sep. 2022, doi: 10.1007/s11042-022-12722-5.

[40] S. Suresh and S. Mohan, "ROI-based feature learning for efficient true positive prediction using convolutional neural network for lung cancer diagnosis," *Neural Comput. Appl.*, vol. 32, no. 20, pp. 15989–16009, Oct. 2020, doi: 10.1007/s00521-020-04787-w.

[41] S. Li, P. Xu, B. Li, L. Chen, Z. Zhou, H. Hao, Y. Duan, M. Folkert, J. Ma, S. Huang, S. Jiang, and J. Wang, "Predicting lung nodule malignancies by combining deep convolutional neural network and handcrafted features," *Phys. Med. Biol.*, vol. 64, no. 17, Sep. 2019, Art. no. 175012, doi: 10.1088/1361-6560/ab326a.

[42] S. Nageswaran, G. Arunkumar, A. K. Bisht, S. Mewada, J. N. V. R. S. Kumar, M. Jawarneh, and E. Asenso, "Lung cancer classification and prediction using machine learning and image processing," *BioMed Res. Int.*, vol. 2022, pp. 1–8, Aug. 2022, doi: 10.1155/2022/1755460.

[43] D. Zhao, Y. Liu, H. Yin, and Z. Wang, "An attentive and adaptive 3D CNN for automatic pulmonary nodule detection in CT image," *Expert Syst. Appl.*, vol. 211, no. 1, pp. 1–24, 2023, doi: 10.1016/j.eswa.2022.118672.

[44] N. Bhaskar and T. S. Ganashree, "Pulmonary nodule detection using Laplacian of Gaussian and deep convolutional neural network," *Smart Innov. Syst. Technol.*, vol. 282, pp. 633–648, Jan. 2022, doi: 10.1007/978-981-16-9669-5_58.

[45] Y. Han, H. Qi, L. Wang, C. Chen, J. Miao, H. Xu, and Z. Wang, "Pulmonary nodules detection assistant platform: An effective computer aided system for early pulmonary nodules detection in physical examination," *Comput. Methods Programs Biomed.*, vol. 217, no. 4, pp. 1–35, 2022.

[46] P. M. Bruntha, S. I. A. Pandian, J. Anitha, S. S. Abraham, and S. N. Kumar, "A novel hybridized feature extraction approach for lung nodule classification based on transfer learning technique," *J. Med. Phys.*, vol. 47, no. 1, pp. 1–9, 2022, doi: 10.4103/jmp.jmp_61_21.

[47] M. Al-Shabi, K. Shak, and M. Tan, "ProCAN: Progressive growing channel attentive non-local network for lung nodule classification," *Pattern Recognit.*, vol. 122, pp. 1–32, Feb. 2022, doi: 10.1016/j.patcog.2021.108309.

[48] H. Huang, Y. Li, R. Wu, Z. Li, and J. Zhang, "Benign-malignant classification of pulmonary nodule with deep feature optimization framework," *Biomed. Signal Process. Control*, vol. 76, Jul. 2022, Art. no. 103701, doi: 10.1016/j.bspc.2022.103701.

[49] S. A. Mahmood and H. A. Ahmed, "An improved CNN-based architecture for automatic lung nodule classification," *Med. Biol. Eng. Comput.*, vol. 60, no. 7, pp. 1977–1986, Jul. 2022, doi: 10.1007/s11517-022-02578-0.

[50] S. Dodia, B. Annappa, and M. A. Padukudru, "A novel artificial intelligence-based lung nodule segmentation and classification system on CT scans," *Commun. Comput. Inf. Sci.*, vol. 1568, pp. 552–564, Jan. 2022, doi: 10.1007/978-3-031-11349-9_48.

[51] J. Lyu, X. Bi, and S. H. Ling, "Multi-level cross residual network for lung nodule classification," *Sensors*, vol. 20, no. 10, pp. 1–14, 2020, doi: 10.3390/s20102837.

IFTIKHAR NASEER received the M.Phil. degree in computer science from Minhaj University, Lahore, Pakistan. He is currently pursuing the Ph.D. degree with the Faculty of Computer Science and Information Technology, Superior University, Lahore. His research interests include fuzzy systems, computational intelligence, machine learning, cloud computing, image processing, intelligent agents, the IoT, and smart city with various publications in international journals and conferences.

SHEERAZ AKRAM received the Master of Science degree in computer science from the Lahore University of Management Sciences (LUMS), Lahore, Pakistan, and the Ph.D. degree in software engineering from the National University of Sciences and Technology (NUST), Islamabad, Pakistan. He is currently with the Information Systems Department, College of Computer and Information Sciences, Imam Mohammad Ibn Saud Islamic University, Riyadh, Saudi Arabia. He is also associated with the Department of Computer Science, Faculty of Computer Science and Information Technology, Superior University, Lahore. He is also a Coordinator and a Senior Member of Intelligent Data Visual Computing Research (IDVCR). He completed his postdoctoral research training with the University of Pittsburgh, USA, and worked on a project funded through Grant U01 HL137159. He has experience of 17 years of working at universities, which includes three years of international research experience. His research interests include data science, medical image processing, artificial intelligence in data science, machine learning, deep learning, computer vision, and digital image processing.

TEHREEM MASOOD received the bachelor's degree (Hons.) from the University of Punjab, the M.S. (Research) degree (Hons.) in software engineering from MAJU Islamabad, and the Ph.D. degree in computing from the Decision and Information Systems for Production Systems (DISP) Laboratory, INSA Lyon, University de Lyon, France. She is currently an academician, a software engineer, a data scientist, a researcher, and an entrepreneur having leadership qualities. She has 14 years of experience, including industry, academia, and research at both national and international levels. She is also a Senior Member of Intelligent Data Visual Computing Research (IDVCR). She is a HEC Approved Ph.D. Supervisor and a recipient of the Erasmus Mundus Scholarship under the Clink Project in France. She was a Senior Software Engineer with Pakistan Air Force in a research and development setup. Her research interests include data science, machine learning, deep learning, software testing, semantic web, and service oriented architecture. She has implemented performance-based semantic, analytical, and predictive models for service sustainability and decision support in SOA following the machine learning approach. She has validated with the implementation of an industrial business process use case and public data set repositories of shared services. She has developed the RWest Tool for specification-based regression testing of web services.

MUHAMMAD RASHID received the Ph.D. degree in computer science from the National University of Computer and Emerging Sciences (NUCES), Pakistan. He is currently serving as Head of the Department, Computer Science at National University of Technology, Islamabad, Pakistan. He has served as the Head of Department (IT) at Rustaq College of Applied Sciences, Oman, from 2012 to August 2018. He Served as an Assistant Professor at Foundation University, Islamabad, Pakistan, from 2010 to March 2012. His research interests include software development, programming, and artificial intelligence.

ARFAN JAFFAR received the M.Sc. degree in computer science from Quaid-i-Azam University, Islamabad, Pakistan, in March 2003, and the M.S. and Ph.D. degrees in computer science from the FAST National University of Computer and Emerging Sciences, in 2006 and 2009, respectively. He received a postdoctoral research fellowship from South Korea and carried-out research at the top raking Korean University, ''Gwangju Institute of Science and Technology, Gwangju, South Korea,'' from 2010 to 2013. He was an Assistant Professor with Al Imam Mohammad Ibn Saud Islamic University, Riyadh, Saudi Arabia, from March 2013 to August 2018. He is currently the Dean of the Faculty of Computer Science and Information Technology, Superior University, Lahore, Pakistan. He is also the Director of Intelligent Data Visual Computing Research (IDVCR). He is a reviewer of 30 reputed international journals, such as IEEE TRANSACTIONS ON PATTERN ANALYSIS AND MACHINE INTELLIGENCE (TPAMI), IEEE TRANSACTIONS ON IMAGE PROCESSING, IEEE TRANSACTIONS ON INDUSTRIAL ELECTRONICS, *Pattern Recognition*, and *Knowledge and Information Sciences*. His research interests include image processing, data science, machine learning, computer vision, artificial intelligence, and medical images.